

Accepted Manuscript

Statistical and Hydrological Evaluation of TRMM-based Multi-satellite Precipitation Analysis over the Wangchu Basin of Bhutan: Are the Latest Satellite Precipitation Products 3B42V7 Ready for Use in Ungauged Basins?

Xianwu Xue, Yang Hong, Ashutosh S. Limaye, Jonathan Gourley, George J. Huffman, Sadiq Ibrahim Khan, Chhimi Dorji, Sheng Chen

PII: S0022-1694(13)00495-2

DOI: <http://dx.doi.org/10.1016/j.jhydrol.2013.06.042>

Reference: HYDROL 18973

To appear in: *Journal of Hydrology*

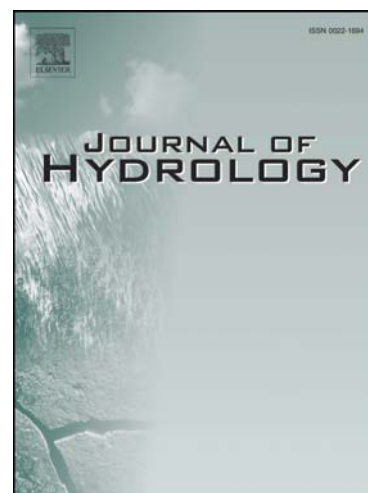
Received Date: 5 October 2012

Revised Date: 6 June 2013

Accepted Date: 23 June 2013

Please cite this article as: Xue, X., Hong, Y., Limaye, A.S., Gourley, J., Huffman, G.J., Khan, S.I., Dorji, C., Chen, S., Statistical and Hydrological Evaluation of TRMM-based Multi-satellite Precipitation Analysis over the Wangchu Basin of Bhutan: Are the Latest Satellite Precipitation Products 3B42V7 Ready for Use in Ungauged Basins?, *Journal of Hydrology* (2013), doi: <http://dx.doi.org/10.1016/j.jhydrol.2013.06.042>

This is a PDF file of an unedited manuscript that has been accepted for publication. As a service to our customers we are providing this early version of the manuscript. The manuscript will undergo copyediting, typesetting, and review of the resulting proof before it is published in its final form. Please note that during the production process errors may be discovered which could affect the content, and all legal disclaimers that apply to the journal pertain.



1
2
3
4
5
6
7
8
9
10
11
12
13
14
15
16
17
18

**Statistical and Hydrological Evaluation of TRMM-based
Multi-satellite Precipitation Analysis over the Wangchu Basin
of Bhutan: Are the Latest Satellite Precipitation Products
3B42V7 Ready for Use in Ungauged Basins?**

Xianwu Xue^{1,2}, Yang Hong^{1,2}, Ashutosh S. Limaye³, Jonathan Gourley⁴, George. J. Huffman⁵, Sadiq Ibrahim Khan¹, Chhimi Dorji⁶ and Sheng Chen¹

1. School of Civil Engineering and Environmental Sciences, University of Oklahoma

2. Advanced Radar Research Center, National Weather Center, Norman, OK 73072

3. ZP11/ Earth Science Office, NASA Marshall Space Flight Center 320 Sparkman Dr.,
Huntsville, AL 35805

4. NOAA/National Severe Storms Laboratory, Norman, OK 73072

5. NASA Goddard Space Flight Center, Greenbelt, MD 20771

6. Department of Hydro-Met Services, Ministry of Economic Affairs, Bhutan

Corresponding author address:

Yang Hong, Atmospheric Radar Research Center, National Weather Center suite 3630,
120 David L. Boren Blvd, Norman, OK 73072-7303

Tel.: 1-405-325-3644; Email: yanghong@ou.edu

19 **Abstract**

20 The objective of this study is to quantitatively evaluate the successive Tropical Rainfall
21 Measuring Mission (TRMM) Multi-satellite Precipitation Analysis (TMPA) products and
22 further to explore the improvements and error propagation of the latest 3B42V7
23 algorithm relative to its predecessor 3B42V6 using the Coupled Routing and Excess
24 Storage (CREST) hydrologic model in the mountainous Wangchu Basin of Bhutan. First,
25 the comparison to a decade-long (2001-2010) daily rain gauge dataset reveals that: 1)
26 3B42V7 generally improves upon 3B42V6's underestimation both for the whole basin
27 (bias from -41.15% to -8.38%) and for a $0.25^{\circ} \times 0.25^{\circ}$ grid cell with high-density gauges
28 (bias from -40.25% to 0.04%), though with modest enhancement of correlation
29 coefficients (CC) (from 0.36 to 0.40 for basin-wide and from 0.37 to 0.41 for grid); and 2)
30 3B42V7 also improves its occurrence frequency across the rain intensity spectrum. Using
31 the CREST model that has been calibrated with rain gauge inputs, the 3B42V6-based
32 simulation shows limited hydrologic prediction NSCE skill (0.23 in daily scale and 0.25
33 in monthly scale) while 3B42V7 performs fairly well (0.66 in daily scale and 0.77 in
34 monthly scale), a comparable skill score with the gauge rainfall simulations. After
35 recalibrating the model with the respective TMPA data, significant improvements are
36 observed for 3B42V6 across all categories, but not as much enhancement for the already-
37 well-performing 3B42V7 except for a reduction in bias (from -26.98% to -4.81%). In
38 summary, the latest 3B42V7 algorithm reveals a significant upgrade from 3B42V6 both
39 in precipitation accuracy (i.e., correcting the underestimation) thus improving its

40 potential hydrological utility. Forcing the model with 3B42V7 rainfall yields comparable
41 skill scores with in-situ gauges even without recalibration of the hydrological model by
42 the satellite precipitation, a compensating approach often used but not favored by the
43 hydrology community, particularly in ungauged basins.

44

45 **Keywords:** CREST Model; A-Priori Parameter Estimation; Hydrologic Modeling
46 Evaluation; Precipitation Estimation

47

ACCEPTED MANUSCRIPT

48 **1 Introduction**

49 Precipitation is among the most important forcing data for hydrological models. It has
50 been arguably nearly impossible for hydrologists to simulate the water cycles over
51 regions with no or sparse precipitation gauge networks, especially over complex terrain
52 or remote areas. Recently, the satellite precipitation products such as TMPA (Huffman et
53 al., 2007), CMORPH (Joyce et al., 2004), PERSIANN (Sorooshian et al., 2000) and
54 PERSIANN-CCS (Hong et al., 2004) are starting to provide alternatives for estimating
55 rainfall data and also pose new challenges for hydrologists in understanding and applying
56 the remotely-sensed information.

57 The Tropical Rainfall Measuring Mission (TRMM) Multi-satellite Precipitation
58 Analysis (TMPA), developed by the National Aeronautics and Space Administration
59 (NASA) Goddard Space Flight Center (GSFC), provides a calibration-based sequential
60 scheme for combining precipitation estimates from multiple satellites, as well as monthly
61 gauge analyses where feasible, at fine spatial and temporal scales ($0.25^{\circ} \times 0.25^{\circ}$ and 3
62 hourly) over 50°N - 50°S (Huffman et al., 2007). TMPA is computed for two products:
63 near-real-time version (TMPA 3B42RT, hereafter referred to as 3B42RT) and post-real-
64 time research version (TMPA 3B42 V6, hereafter referred to as 3B42V6). 3B42V6 has
65 been widely used in hydrological applications (Bitew and Gebremichael, 2011; Bitew et
66 al., 2011; Khan et al., 2011a; Khan et al., 2011b; Li et al., 2012; Stisen and Sandholt,
67 2010; Su et al., 2008), however, its computation ended June 30th 2011 and 3B42V6 was
68 replaced by the new version (TMPA 3B42 V7, hereafter referred to as 3B42V7), which

69 has been reprocessed and available from 1998 to present. Previously, 3B42V6 has been
70 validated by several studies (Bitew and Gebremichael, 2011; Bitew et al., 2011;
71 Chokngamwong and Chiu, 2008; Islam and Uyeda, 2007; Jamandre and Narisma; Jiang
72 et al., 2012; Li et al., 2012; Mishra et al., 2010; Stisen and Sandholt, 2010; Su et al., 2008;
73 Yong et al., 2012; Yong et al., 2010), while the newly available 3B42V7 is evaluated in
74 tropical cyclone systems (Chen et al., 2013b) and the United States (Chen et al. 2013a
75 and Kirstetter et al. 2013), it has not been extensively statistically and hydrologically
76 validated in mountainous South Asian regions..

77 Therefore, the objectives of this study are designed (1) to evaluate the widely used
78 globally-available, high-resolution TMPA satellite precipitation products over the
79 mountainous medium-sized Wangchu basin (3550 km²) in Bhutan, and more importantly
80 (2) to assess improvements of the latest upgrade version (3B42V7) relative to its
81 predecessor in terms of statistical performance and hydrologic utility. Additionally, this
82 study aims to shed light on the suitability of recalibrating a hydrological model with the
83 remotely-sensed rainfall information. The remainder of this paper is organized as follows:
84 Section 2 introduces the study area, the datasets used, and the methodology, including a
85 brief description of the CREST distributed hydrological model and its upgrade to the new
86 version (CREST Version 2.0). The results are discussed in Section 3, and then Section 4
87 draws the conclusions of this study.

88

89 2 Study Area, Data and Methodology

90 2.1 Study Area

91 The Wangchu Basin, with a total drainage area of approximately 3550 km² is located
92 within 89°6'- 89°46'E and 27°6'-27°51'N in the west of Bhutan (Figure 1). Wangchu
93 Basin is the most populous part of the country with about 3/5 of the population living in
94 1/5 of the basin area. The basin is equipped with one streamflow gauge at the outlet
95 Chhukha Dam Hydrological station and five rain gauge stations. The soil types are
96 dominated by Sandy Clay Loam (75.1%) and Loam (24.9%) based on the Harmonized
97 World Soil Database (HWSD v1.1) (FAO/IIASA/ISRIC/ISSCAS/JRC, 2009). The
98 various vegetation types of this basin are composed of evergreen needleleaf forest
99 (48.1%), woodland (17.8%), open shrubland (9.7%), wooded grassland (8.2%), grassland
100 (7.6%) and other land-use types (less than 10%) (Hansen et al., 2000).

101 The northern periphery of the Wangchu Basin in the Himalayas has elevations over
102 6000 m and maintains an annual snowpack. Lower portions of the basin are drastically
103 different and are subject to a summer monsoon from May to October (Bookhagen and
104 Burbank, 2010). On average, the annual month with the greatest precipitation is July or
105 August with 161 to 546 mm/month based on the five rain gauge station data shown in
106 (Table 1), and the largest resulting streamflow occurs in June or August with 251m³s⁻¹. It
107 is possible that snowmelt contributes to a portion of this peak streamflow, but the
108 majority is driven by the summer monsoon rains. In this study, neither the precipitation
109 products nor the model explicitly deal with frozen precipitation. These are subjects

110 requiring additional investigation, especially in light of the forthcoming Global
111 Precipitation Measurement Mission (GPM), which aims to quantitatively estimate frozen
112 precipitation amounts.

113 **Insert Figure 1 about Here**

114

115 **2.2 In-situ and Satellite Precipitation Datasets**

116 **2.2.1 Gauged Precipitation and Discharge Data**

117 Daily observed precipitation data are obtained from the Hydro-Met Services
118 Department of Bhutan from 2001 to 2010 for the 5 rain gauge stations located within the
119 Wangchu basin. In winter, frozen precipitation is reported in the form of water equivalent
120 and computed by melting the ice/snow with hot water in the standard vessel and
121 deducting the hot water volume from the total volume. The Thiessen polygon method is
122 used to interpolate the rain gauge data to the spatial distributed grid data fitting the model
123 grid resolution (30 arc-second) (Figure 1). We also obtained the daily discharge data at
124 the basin outlet for the same time period.

125 **2.2.2 TMPA 3B42 Research Products**

126 TMPA precipitation products are available in two versions: near-real-time version
127 (3B42RT) and post-real-time research version (3B42) adjusted by monthly rain gauge
128 data. The 3B42 products have two successive versions: version 6 and the latest version 7
129 (3B42V6 and 3B42V7). In this study, we evaluated and compared the two high-resolution
130 (3 hours and $0.25^{\circ} \times 0.25^{\circ}$) satellite precipitation products: 3B42V6 and 3B42V7.

131 The TMPA algorithm (Huffman et al., 2007) calibrates and combines microwave (MW)
132 precipitation estimates, and then creates the infrared precipitation (IR) estimates using the
133 calibrated MW. After this, it combines the MW and IR estimates to create the TMPA
134 precipitation estimates. MW data used in Version 6 are from the TRMM Microwave
135 Imager (TMI), Special Sensor Microwave Imager (SSM/I) F13, F14 and F15 on Defense
136 Meteorological Satellite Program (DMSP) satellites, and the Advanced Microwave
137 Scanning Radiometer-Earth Observing System (AMSR-E) on Aqua, and the Advanced
138 Microwave Sounding Unit-B (AMSU-B) N15, N16 and N17 on the NOAA satellite; IR
139 data collected by geosynchronous earth orbit (GEO) satellites, GEO-IR. The 3B42V6
140 also use other data sources: TRMM Combined Instrument (TCI) employed from TMI and
141 PR, monthly rain gauge data from GPCP ($1^{\circ} \times 1^{\circ}$) and the Climate Assessment and
142 Monitoring System (CAMS) $0.5^{\circ} \times 0.5^{\circ}$ developed by CPC. Based on the lessons learned
143 in 3B42V6, 3B42V7 includes consistently reprocessed versions for the data sources used
144 in 3B42V6 and introduces additional datasets, including the Special Sensor Microwave
145 Imager/Sounder (SSMIS) F16-17 and Microwave Humidity Sounder (MHS) (N18 and
146 N19) and Meteorological Operational satellite programme (MetOp) and the 0.07° Grsat-
147 BI infrared data. All of these data can be freely downloaded from the website:
148 <http://trmm.gsfc.nasa.gov/> and <http://mirador.gsfc.nasa.gov>.

149 **2.2.3 Evapotranspiration**

150 The potential evapotranspiration (PET) data used in this study are from the global daily
151 potential evapotranspiration database provided by the Famine Early Warning Systems

152 Network (hereafter referred as FEWSPET) global data portal (see
153 <http://earlywarning.usgs.gov/fews/global/web/readme.php?symbol=pt>). FEWSPET is
154 calculated from the climate parameter extracted from global data assimilation system
155 (GDAS) analysis fields, has 1-degree resolution, and covers the entire globe from 2001 to
156 the present.

157 **2.3 CREST Model**

158 The Coupled Routing and Excess Storage (CREST) Model (Khan et al., 2011a; Khan et
159 al., 2011b; Wang et al., 2011) is a grid-based distributed hydrological model developed
160 by the University of Oklahoma (<http://hydro.ou.edu>) and NASA SERVIR Project Team
161 (www.servir.net). It computes the runoff generation components (e.g., surface runoff and
162 infiltration) using the variable infiltration capacity curve (VIC), a concept originally
163 contained in the Xinanjiang Model (Zhao, 1992; Zhao et al., 1980) and later represented
164 in the VIC Model (Liang et al., 1994; Liang et al., 1996). Multi-linear reservoirs are used
165 to simulate cell-to-cell routing of surface and subsurface runoff separately. The CREST
166 model couples the runoff generation component and cell-to-cell routing scheme described
167 above, to reproduce the interaction between surface and subsurface water flow processes.
168 Besides the hydrologic and basic data (DEM, flow direction, flow accumulation, slope
169 etc.), the CREST model employs gridded precipitation and potential evapotranspiration
170 (PET) data as its forcing data. CREST Version 1.6 model has been applied at both global
171 (Wu et al., 2012) and regional scales (Khan et al., 2011a; Khan et al., 2011b) (more
172 applications can be found at website: <http://eos.ou.edu> and <http://www.servir.net>).

173 The CREST model used in this study is the upgraded version CREST V2.0. The main
174 features of the latest version are: 1) enhancement of the computation capability using
175 parallel distribution techniques to make the model more efficient than the previous
176 version (Wang et al., 2011); 2) model implementation with options of either spatially
177 uniform, semi-distributed, or distributed parameter values; 3) automatic extraction of *a-*
178 *priori* model parameter estimates from high-resolution land cover and soil texture data.
179 The physically-based parameters, K_{sat} and WM, can be derived from land cover types and
180 soil texture data based on a look-up table (Chow et al., 1988); 4) a modular design
181 framework to accommodate research, development and system enhancements (see Figure
182 2 (a)); and 5) inclusion of the optimization scheme SCE-UA (Duan et al., 1992; Duan et
183 al., 1993) to enable automatic calibration of the CREST model parameters (see Figure 2
184 (a)). Table 1 shows 11 parameters and their descriptions, ranges and default values.
185 Figure 2 (b) shows the vertical profile of hydrological processes in a grid cell. It shows
186 the precipitation is intercepted by a canopy to generate throughfall, and then the
187 throughfall is separated into surface runoff and infiltration components by the variable
188 infiltration curve. Finally, two linear reservoirs are employed to simulate sub-grid cell
189 routing.

190

191

Insert Figure 2 about Here

192

Insert Table 1 about Here

193

194 **2.4 Evaluation Statistics**

195 In order to quantitatively analyze the performance of 3B42V6 and 3B42V7
 196 precipitation products against rain gauge observations and the effect on streamflow
 197 simulation, three widely used validation statistical indices were selected in this study. The
 198 relative Bias (%) was used to measure the agreement between the averaged value of
 199 simulated data (in this study, we call both TMPA products and simulated streamflow as
 200 “simulated data”, “SIM” was used in the formulae) and observed data (such as rain gauge
 201 and observed streamflow in this study, “OBS” was used in the formulae). The root mean
 202 square error (RMSE) was selected to evaluate the average error magnitude between
 203 simulated and observed data. We also use correlation coefficient (CC) to assess the
 204 agreement between simulated and observed data.

$$205 \quad Bias = \left[\frac{\sum_{i=1}^n SIM_i - \sum_{i=1}^n OBS_i}{\sum_{i=1}^n OBS_i} \right] \times 100 \quad (1)$$

$$206 \quad RMSE = \sqrt{\frac{\sum_{i=1}^n (OBS_i - SIM_i)^2}{n}} \quad (2)$$

$$207 \quad CC = \frac{\sum_{i=1}^n (OBS_i - \overline{OBS})(SIM_i - \overline{SIM})}{\sqrt{\sum_{i=1}^n (OBS_i - \overline{OBS})^2 \sum_{i=1}^n (SIM_i - \overline{SIM})^2}} \quad (3)$$

208 Where n is the total number of pairs of simulated and observed data; i is the i th values of
 209 the simulated and observed data; \overline{SIM} and \overline{OBS} are the mean values of simulated and

210 observed data respectively. Nash-Sutcliffe Coefficient of Efficiency (NSCE) is also used
 211 to assess the performance of model simulation and observation.

$$212 \quad NSCE = 1 - \frac{\sum_{i=1}^n (OBS_i - SIM_i)^2}{\sum_{i=1}^n (OBS_i - \overline{OBS})^2} \quad (4)$$

213 **3 Results and Discussion**

214 **3.1 Comparison of Precipitation Inputs**

215 To better understand the impact of precipitation inputs on hydrologic models, the
 216 accuracy of the satellite precipitation against the in-situ rain gauge observations should be
 217 assessed first. This section compares the TMPA and gauge observations over the time
 218 span of January 1, 2001 to December 31, 2010 considering the basin-average
 219 precipitation and within a grid cell containing the dense rain gauge observations (Figure
 220 1). Figure 3 shows that both 3B42V6 and 3B42V7 systematically underestimate, though
 221 at different levels, with biases of -41.15% and -8.38% and CCs of 0.36 and 0.40 at daily
 222 scale, respectively. Similar statistics are found at 0.25° grid-cell scale. Figure 4 indicates
 223 that 3B42V6 largely underestimates with a bias of -40.25% and low CC of 0.37, while
 224 3B42V7 has practically no bias (0.04%) and a relatively higher CC value 0.41.

225

226

Insert Figure 3 about Here

227

228

Insert Figure 4 about Here

229

230 Figures 3d and 4d present the inter-comparison of monthly precipitation estimates to
231 gain further information about the precision and variations at longer time scales. The
232 monthly data for both basin-based and grid cell-based analyses were accumulated from
233 daily data over the same time span from January 2001 to December 2010. At monthly
234 time scale, both the basin-based and grid cell-based data show that 3B42V7 has better
235 agreement with the monthly rain gauge data. Both Figure 3 and Figure 4 indicate that the
236 latest V7 algorithm significantly corrects the underestimation bias in its predecessor
237 version V6.

238 Figure 5 (a) and (b) show the frequency distribution of daily precipitation for different
239 precipitation intensities (PI) for the basin-averaged and the grid cell-based precipitation
240 time series, respectively. Figure 5 (a) shows that for the basin-averaged data, both
241 3B42V6 and 3B42V7 overestimate at the low PI range (less than 5 mm/day), but they
242 underestimate at the medium and high PI ranges. However, 3B42V7 is in better
243 agreement with the rain gauge observations than 3B42V6 for the basin-averaged
244 comparison across all PIs. Similarly, better agreement has been found in Figure 5 (b) for
245 the new Version-7 products at the grid cell scale, except for values greater than 30
246 mm/day where there is overestimation.

247

248

Insert Figure 5 about Here

249

250 3.2 Streamflow Simulation Scenarios

251 Although different precipitation products vary in accuracy and spatiotemporal
252 resolutions, they might have similar hydrological prediction (i.e., streamflow simulation)
253 skill after re-calibrating the model using the respective precipitation products (Jiang et al.,
254 2012; Stisen and Sandholt, 2010). In the previous section, we compared the 3B42V6 and
255 3B42V7 precipitation products against the rain gauge observations; the next step is to
256 evaluate how these two TMPA products affect streamflow simulations. Their hydrological
257 evaluation is performed under two scenarios:

258 I. In-situ gauge benchmarking: Calibrate the CREST model with five years of rain
259 gauge data (January 2001 through December 2005). Then, replace the rain gauge
260 forcing with precipitation from 3B42V6 and 3B42V7 for an independent
261 validation period from January 2006 through December 2010 using the rain
262 gauge-calibrated model parameters.

263 II. Product-specific calibration: Recalibrate the CREST model using the 3B42V6 and
264 3B42V7 precipitation data, respectively, over the same calibration period and then
265 use the product-specific parameter sets to simulate streamflow over the same
266 validation period as Scenario I.

267 Scenario I, gauge benchmarking, is widely used by the hydrological community
268 especially over gauged basins, while Scenario II is arguably deemed as an alternative for
269 application to ungauged basins where only rainfall from remote-sensing platforms are
270 available for use.

271

272 **3.2.1 Scenario I: CREST Benchmarked by In-situ Gauge Data**273 **1) Rain Gauge Calibration and Validation**

274 The CREST model parameters are calibrated using rain gauge inputs for the period
275 from January 2001 to December 2005 using the automatic calibration method (SCE-UA)
276 by maximizing the NSCE value between the simulated and observed daily streamflow.
277 The calibrated model is subsequently validated for the period from January 2006 to
278 December 2010. Figure 6 compares the simulated streamflow forced by rain gauge data
279 with the observed streamflow in terms of time series plots and exceedance probability
280 plots at daily and monthly scales. Figure 6 (a) and (b) show that general agreement exists
281 between the observed and simulated streamflow. However, the simulated streamflow
282 consistently underestimates the peaks, especially in the validation period and in relatively
283 low flow seasons as well. The exceedance probabilities in Figure 6 (c) and (d) also show
284 underestimation at low and high streamflow observations, while the simulations match
285 relatively well in the intermediate ranges. As summarized in Table 2 and Table 3, the
286 statistical indices show that there is very good agreement between the simulated and
287 observed hydrographs in the calibration period for both daily and monthly time scale, and
288 reasonable simulations occurred in the validation period as well. Based on the criteria of
289 the statistical indices in Moriasi et al. (2007), the model calibration and validation results
290 indicate that the CREST model is well benchmarked by the in-situ data at the daily and
291 monthly time scale, so it can be used to evaluate the utility of the satellite precipitation

292 products for hydrological prediction (i.e., streamflow) in this basin.

293 **Insert Figure 6 about Here**

294 **Insert Table 2 about Here**

295 **Insert Table 3 about Here**

296 **2) Impacts of satellite precipitation forcing**

297 The gauge-benchmarked model is then forced by the TMPA 3B42V6 and 3B42V7
298 products from 2001 to 2010 using the model parameters calibrated by rain gauge data
299 during the period from 2001 to 2005. Figure 7 and Figure 8 compare the daily and
300 monthly time series of the simulated and observed hydrographs for both the calibration
301 and validation periods. While 3B42V6 largely missed the high peak flows at both daily
302 and monthly time series, 3B42V7 adequately captured a majority of the peak flows,
303 especially at the smoothed monthly scale. The daily and monthly statistical comparisons
304 in Table 2 and Table 3 show that the daily and monthly simulations forced by rain gauge
305 data had better skill (NSCE=0.76/0.91, BIAS=-9.73%/-9.75%, CC=0.89/0.96) than those
306 based on 3B42V6 and 3B42V7 in the calibration period, which is expected. Interestingly,
307 the 3B42V7-forced model simulations had very similar to and slightly better performance
308 compared to the rain gauge-forced simulations in the validation period. A likely
309 explanation is one of the rain gauge stations (i.e. the Dochula) had missing data from
310 September 2006 to December 2010, which apparently degrades the hydrologic skill of
311 this product. Overall, simulations forced by 3B42V7 were a significant improvement
312 over 3B42V6. This clearly shows the improvements of the new version-7 algorithm upon

313 its predecessor V6 products both statistically and now hydrologically.

314

315

Insert Figure 7 about Here

316

317 **3.2.2 Scenario II: CREST calibrated by individual TMPA products**

318 To further assess the effects of TMPA 3B42 (V6 and V7) products on streamflow,
319 the CREST model is recalibrated and validated with 3B42V6 and 3B42V7 for the same
320 period as Scenario I. This scenario is often used as an alternative strategy for remote
321 sensing precipitation over ungauged basins. As shown in Figure 8, all simulations are
322 significantly improved after the recalibration, and they capture most of the daily and
323 monthly peak flows. Comparatively, the CREST model simulations based on 3B42V7
324 inputs have better skill than those based on 3B42V6. As summarized in Table 2 and Table
325 3, simulations have good statistical agreement with observed streamflow at daily and
326 monthly scale.

327 The statistical indices of daily NSCE, Bias and CC in Table 2 were selected for
328 visual comparison of the two modeling scenarios. Figure 9 indicates that the product-
329 specific recalibration in Scenario II has obviously improved the NSCE and CC values
330 and reduced the Bias values for both the calibration and validation periods. It is noted that
331 the recalibration forcing with 3B42V7 in Scenario II has much higher NSCE and smaller
332 Bias than 3B42V6, and very comparable CC values, all of which improved upon the rain
333 gauge-benchmarked model.

334

335 **3.3 Discussion of parameter compensation effect from Scenario II**

336 Table 4 shows the optimum parameter sets forced by 3B42V6 and 3B42V7, relative
337 to the gauge forcing, for the calibration period from 2001 to 2005 using the SCE-UA
338 algorithm. Note that the parameter values of Ksat and WM are spatially distributed but
339 have been basin-averaged and summarized in Table 4. It shows that 3B42V7-calibrated
340 parameters have less deviation from the gauge-calibrated parameter values than 3B42V6.
341 For example, RainFact is the adjustment factor of the precipitation either due to canopy
342 interception or bias. Table 4 shows that 3B42V6 increases the RainFact value from 0.87
343 to 1.34, to compensate its underestimation as shown in Figure 3 and Figure 4, while
344 3B42V7's estimated value (0.98) is closer to 1 and the Gauge value (0.87). Another
345 example is KE, the ratio of potential evapotranspiration to the satellite PET data. Table 4
346 reveals that 3B42V6 demands a reduced KE value from 0.10 to 0.05 in order to partition
347 more precipitation into runoff while 3B42V7 only slightly increases it from 0.10 to 0.13,
348 possibly to partially offset the above RainFact increase, amongst other parametric
349 interactions. The third example is Ksat, the soil saturated hydraulic conductivity. Table 4
350 shows that the Ksat of 3B42V6 reduced from 56.90 to 33.09 while V7 only changed
351 slightly from 56.90 to 52.73. Regarding the mean water capacity, WM, 3B42V6
352 decreased from 166.50 to 142.71 to hold less water in the soils while 3B42V7 did not
353 change much from the gauge-calibrated value, which is presumably closer to the truth. It
354 also shows the overland flow coefficient, $coeM$, the average channel flow speed, $coeR$,

355 the overland flow recession coefficient, K_S , and the interflow recession coefficient, K_I ,
356 all had reduced values to retain more water in the river basin after recalibrating the
357 parameters to both of the satellite products. Not surprisingly, Table 4 also shows some
358 opposite changes of values such as K_E for 3B42V7 and $coeS$, the surface-interflow
359 conversion factor, for both 3B42V6 and 3B42V7, resulting in a slight decrease in
360 streamflow.

361 In addition to the analysis of the parameters properties, water balance analysis is
362 another important indicator for analyzing the effect of the parameter recalibration. Thus
363 the difference of water balance components over 10-year (2001-2010) simulations is
364 further examined using rain gauge and TMPA 3B42 rainfall, respectively. In CREST
365 model, the water balance budgeting partitions the precipitation after canopy interception
366 into actual evapotranspiration (ET), runoff depth (i.e. streamflow) and water storage
367 change (ΔS), as shown in Figure 10. As expected, precipitation is the dominant runoff
368 generation input so in Figure 3, all satellite rainfall forced simulations underestimated the
369 streamflow compared to rain gauge results in scenario I. However, in scenario II, the
370 model was recalibrated with respective satellite rainfall, the increased partition of the
371 satellite driven streamflow simulations comes at the expense of a significant decrease of
372 water storage due to the effect of the parameters value changes (shown in figure 10). In
373 the gauge rainfall driven simulations, 27.90% of precipitation will be stored in this basin,
374 however, 26.43% (27.18%) of precipitation is water storage in scenario I while 8.95%
375 (16.09%) in scenario II for 3B42V6 (3B42V7).

376 From the above discussion, it is clear that the overall effect of the recalibrated
377 parameter sets is to largely compensate for rainfall underestimation in 3B42V6 while less
378 so for 3B42V7. The effect of arriving at a very similar simulation with different
379 combinations of parameter settings has been called “Equifinality” of the hydrological
380 model (Aronica et al., 1998; Beven and Freer, 2001; Zak and Beven, 1999). This study
381 clearly shows how different parameter settings can compensate for errors in the satellite
382 rainfall forcing and can thus improve model predictions of streamflow. It is possible that
383 the current model structural deficiency, i.e., not accounting for snowmelt process, is
384 compensated by the model re-calibration. However, this parameter compensation effect
385 comes with the price of having a locally optimized model with parameter values
386 unrepresentative of reality. This might limit the model’s predictive capability at internal
387 sub-basins, or under different initial conditions. This is particularly concerning under
388 scenarios involving climate change. In any case, the recalibration strategy could be
389 especially problematic for 3B42V6 (Bitew and Gebremichael, 2011; Jiang et al., 2012),
390 however the 3B42V7 product gives higher confidence for use in ungauged basins even
391 without the need for recalibration.

392

393

Insert Table 4 about Here

394

395

396 **4 Summary and Conclusions**

397 Satellite precipitation products are very important for regional and global
398 hydrological studies, particularly for remote regions and developing countries. This study
399 first focuses on statistically assessing the accuracy of the TMPA 3B42V6 product vs. its
400 latest successive version 3B42V7, and then hydrologically evaluates their streamflow
401 prediction utility using the CREST distributed hydrologic model in the mountainous
402 Wangchu Basin of Bhutan.

403 The two versions of TMPA satellite products are statistically compared with a
404 decade-long (2001-2010) rain gauge dataset at daily and monthly scales. In general,
405 3B42V7 consistently improves upon 3B42V6's underestimation both for the whole basin
406 (bias improved from -41.15% to -8.38%) and for a $0.25^{\circ} \times 0.25^{\circ}$ grid cell with high-
407 density gauges (bias improved from -40.25% to 0.04%), though with modest
408 enhancement of correlation coefficients (CC) (from 0.36 to 0.40 for entire basin and from
409 0.37 to 0.41 for the grid cell). 3B42V7 also improves upon 3B42V6 in terms of
410 occurrence frequency across the rain intensity spectrum. Apparently the results show that
411 the new algorithm 3B42V7 has much improved accuracy upon 3B42V6, in concert with
412 other studies in different areas (Chen et al. 2013ab and Kirstetter et al. 2013). The
413 improvement from V6 to V7 is mainly a combination of three factors: 1) the enhanced
414 TMPA Level-2 retrieval algorithms (Chen et al. 2013a and Kirstetter et al. 2013), 2)
415 incorporation of the global gauge network (i.e. GPCC) data with improved climatology
416 and anomaly analysis (Huffman et al., 2011), and 3) additional satellite observations

417 incorporated (Huffman and Bolvin, 2012)..

418 For the hydrological evaluation, two scenario-based calibration and validation
419 experiments are conducted over the same 10-year time span. Scenario I, in-situ gauge
420 benchmarking, is widely used by the hydrological community especially over gauged
421 basins, while Scenario II, input-specific recalibration, is arguably deemed as an
422 alternative for application to ungauged basins where only remote-sensing rainfall data
423 may be available for use. In Scenario I, the 3B42V6-based simulation shows lower
424 hydrologic prediction skill in terms of NSCE (0.23 at daily scale and 0.25 at monthly
425 scale) while 3B42V7 performs fairly well (0.66 at daily scale and 0.77 at monthly scale),
426 a comparable skill score with the simulations using the gauge benchmark. For the
427 precipitation-specific calibration in Scenario II, significant improvements are observed
428 for 3B42V6 across all statistics. These enhancements are not as obvious for the already-
429 well-performing 3B42V7-calibrated model, except for some reduction in bias (from -
430 26.98% to -4.81%). This behavior is consistent with previous studies (Bitew and
431 Gebremichael, 2011; Bitew et al., 2011; Jiang et al., 2012). This study offers unique
432 insights into 3B42V6 and 3B42V7 products in a mountainous South Asian basin.

433 In concert with several other studies by Chen et al 2013a and Kirstetter et al 2013 in
434 the US and Chen et al 2013b in the tropics, this study also reveals the latest 3B42V7
435 algorithm has a noticeable improvements from 3B42V6 both in terms of accuracy (i.e.,
436 correcting the underestimation) and in its promising hydrological, even with or without
437 recalibration of the hydrological model with respective rainfall inputs. The parameter

438 compensation effect is often recognized but still used by the hydrology community. This
439 approach has been noted to be problematic due to unrealistic parameter settings which
440 may ultimately limit the model's predictive capability under conditions of climate change
441 and differing initial conditions.

442

443 **Acknowledgements**

444 The current study was supported by the NASA/Marshall Space Flight Center Grants
445 NNM11AB34P and NNMi2428088Q to the University of Oklahoma.

446

447 **References**

448 Aronica, G., Hankin, B. and Beven, K.J., 1998. Uncertainty and equifinality in calibrating
449 distributed roughness coefficients in a flood propagation model with limited data.

450 *Advances In Water Resources*, 22(4): 349-365.

451 Beven, K.J. and Freer, J., 2001. Equifinality, data assimilation, and uncertainty estimation

452 in mechanistic modelling of complex environmental systems using the GLUE

453 methodology. *Journal Of Hydrology*, 249(1-4): 11-29.

454 Bitew, M.M. and Gebremichael, M., 2011. Evaluation of satellite rainfall products

455 through hydrologic simulation in a fully distributed hydrologic model. *Water*

456 *Resources Research*, 47(6): W06526.

457 Bitew, M.M., Gebremichael, M., Ghebremichael, L.T. and Bayissa, Y.A., 2011.

458 Evaluation of High-Resolution Satellite Rainfall Products through Streamflow

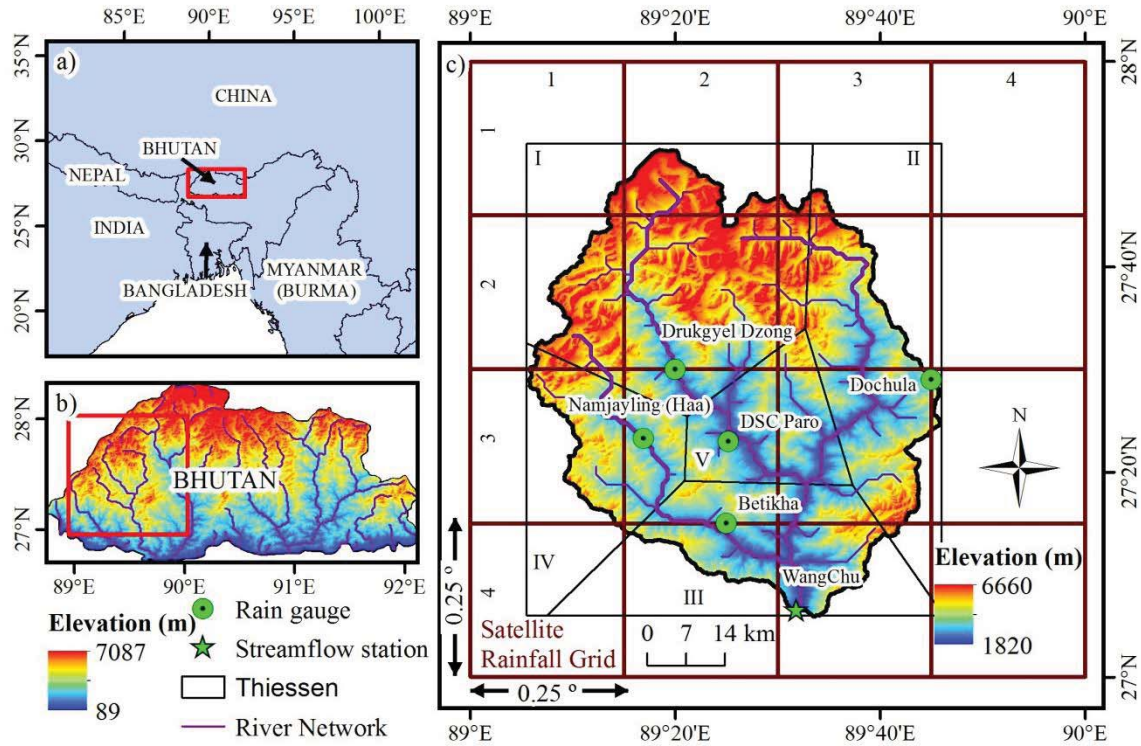
- 459 Simulation in a Hydrological Modeling of a Small Mountainous Watershed in
460 Ethiopia. *Journal Of Hydrometeorology*, 13(1): 338-350.
- 461 Bookhagen, B. and Burbank, D.W., 2010. Toward a complete Himalayan hydrological
462 budget: Spatiotemporal distribution of snowmelt and rainfall and their impact on
463 river discharge. *J. Geophys. Res.*, 115(F3): F03019.
- 464 Chen, Sheng et al., 2013a. Evaluation of the Successive V6 and V7 TRMM Multi-
465 satellite Precipitation Analysis Over the Continental United States. *Water*
466 *Resources Research*. (Conditionally accepted)
- 467 Chen, Y., Ebert, E.E., Walsh, K.J.E. and Davidson, N.E., 2013b. Evaluation of TRMM
468 3B42 Precipitation Estimates of Tropical Cyclone Rainfall using PACRAIN Data.
469 *Journal of Geophysical Research: Atmospheres*, doi: 10.1002/jgrd.50250
470 (accepted for publication) .
- 471 Chokngamwong, R. and Chiu, L.S., 2008. Thailand Daily Rainfall and Comparison with
472 TRMM Products. *Journal of Hydrometeorology*, 9(2): 256-266.
- 473 Chow, V.T., Maidment, D.R. and Mays, L.W., 1988. *Applied Hydrology*. McGraw-Hill
474 series in water resources and environmental engineering. McGraw-Hill, Inc., New
475 York.
- 476 Duan, Q., Sorooshian, S. and Gupta, V., 1992. Effective and efficient global optimization
477 for conceptual rainfall-runoff models. *Water Resour. Res.*, 28(4): 1015-1031.
- 478 Duan, Q.Y., Gupta, V.K. and Sorooshian, S., 1993. Shuffled complex evolution approach
479 for effective and efficient global minimization. *Journal of Optimization Theory*

- 480 and Applications, 76(3): 501-521.
- 481 FAO/IIASA/ISRIC/ISSCAS/JRC, 2009. Harmonized World Soil Database (version 1.1),
482 FAO, Rome, Italy and IIASA, Laxenburg, Austria.
- 483 Hansen, M.C., Defries, R.S., Townshend, J.R.G. and Sohlberg, R., 2000. Global land
484 cover classification at 1 km spatial resolution using a classification tree approach.
485 International Journal Of Remote Sensing, 21(6): 1331 - 1364.
- 486 Hong, Y., Hsu, K.-L., Sorooshian, S. and Gao, X., 2004. Precipitation Estimation from
487 Remotely Sensed Imagery Using an Artificial Neural Network Cloud
488 Classification System. Journal Of Applied Meteorology, 43(12): 1834-1853.
- 489 Huffman, G.J., Bolvin, D.T., Nelkin, E. and Adler, R.F., 2011. Highlights of Version 7
490 TRMM Multi-satellite Precipitation Analysis (TMPA). In: C.K.a.G.H. Eds
491 (Editor), 5th Internat. Precip. Working Group Workshop, Workshop Program and
492 Proceedings. Reports on Earth Sys. Sci., 100/2011, Max-Planck-Institut für
493 Meteorologie, Hamburg, Germany.
- 494 Huffman, G. J., and D. T. Bolvin, 2012. TRMM and other data precipitation data set
495 documentation, Laboratory for Atmospheres, NASA Goddard Space Flight Center
496 and Science Systems and Applications.
- 497 Huffman, G.J. et al., 2007. The TRMM Multisatellite Precipitation Analysis (TMPA):
498 Quasi-Global, Multiyear, Combined-Sensor Precipitation Estimates at Fine Scales.
499 Journal of Hydrometeorology, 8(1): 38-55.
- 500 Islam, M.N. and Uyeda, H., 2007. Use of TRMM in determining the climatic

- 501 characteristics of rainfall over Bangladesh. Remote Sensing of Environment,
502 108(3): 264-276.
- 503 Jamandre, C.A. and Narisma, G.T., Spatio-temporal validation of satellite-based rainfall
504 estimates in the Philippines. Atmospheric Research(0).
- 505 Jiang, S. et al., 2012. Comprehensive evaluation of multi-satellite precipitation products
506 with a dense rain gauge network and optimally merging their simulated
507 hydrological flows using the Bayesian model averaging method. Journal of
508 Hydrology, 452-453(0): 213-225.
- 509 Joyce, R.J., Janowiak, J.E., Arkin, P.A. and Xie, P., 2004. CMORPH: A Method that
510 Produces Global Precipitation Estimates from Passive Microwave and Infrared
511 Data at High Spatial and Temporal Resolution. Journal Of Hydrometeorology,
512 5(3): 487-503.
- 513 Khan, S.I. et al., 2011a. Hydroclimatology of Lake Victoria region using hydrologic
514 model and satellite remote sensing data. Hydrol. Earth Syst. Sci., 15(1): 107-117.
- 515 Khan, S.I. et al., 2011b. Satellite Remote Sensing and Hydrologic Modeling for Flood
516 Inundation Mapping in Lake Victoria Basin: Implications for Hydrologic
517 Prediction in Ungauged Basins. Geoscience and Remote Sensing, IEEE
518 Transactions on, 49(1): 85-95.
- 519 Li, X.-H., Zhang, Q. and Xu, C.-Y., 2012. Suitability of the TRMM satellite rainfalls in
520 driving a distributed hydrological model for water balance computations in
521 Xinjiang catchment, Poyang lake basin. Journal Of Hydrology, 426-427(0): 28-38.

- 522 Liang, X., Lettenmaier, D.P., Wood, E.F. and Burges, S.J., 1994. A simple hydrologically
523 based model of land surface water and energy fluxes for general circulation
524 models. *J. Geophys. Res.*, 99(D7): 14415-14428.
- 525 Liang, X., Wood, E.F. and Lettenmaier, D.P., 1996. Surface soil moisture
526 parameterization of the VIC-2L model: Evaluation and modification. *Global and*
527 *Planetary Change*, 13(1–4): 195-206.
- 528 Mishra, A., Gairola, R.M., Varma, A.K. and Agarwal, V.K., 2010. Remote sensing of
529 precipitation over Indian land and oceanic regions by synergistic use of
530 multisatellite sensors. *J. Geophys. Res.*, 115(D8): D08106.
- 531 Moriasi, D.N. et al., 2007. Model Evaluation Guidelines For Systematic Quantification
532 Of Accuracy In Watershed Simulations. *ASABE*, 50(3): 885-900.
- 533 Sorooshian, S. et al., 2000. Evaluation of PERSIANN System Satellite–Based Estimates
534 of Tropical Rainfall. *Bulletin of the American Meteorological Society*, 81(9):
535 2035-2046.
- 536 Stisen, S. and Sandholt, I., 2010. Evaluation of remote-sensing-based rainfall products
537 through predictive capability in hydrological runoff modelling. *Hydrological*
538 *Processes*, 24(7): 879-891.
- 539 Su, F., Hong, Y. and Lettenmaier, D.P., 2008. Evaluation of TRMM Multisatellite
540 Precipitation Analysis (TMPA) and Its Utility in Hydrologic Prediction in the La
541 Plata Basin. *Journal of Hydrometeorology*, 9(4): 622-640.
- 542 Wang, J. et al., 2011. The coupled routing and excess storage (CREST) distributed

- 543 hydrological model. *Hydrological Sciences Journal*, 56(1): 84-98.
- 544 Wu, H., Adler, R.F., Hong, Y., Tian, Y. and Policelli, F., 2012. Evaluation of Global Flood
545 Detection Using Satellite-Based Rainfall and a Hydrologic Model. *Journal of*
546 *Hydrometeorology*, 13(4): 1268-1284.
- 547 Yong, B. et al., 2012. Assessment of evolving TRMM-based multisatellite real-time
548 precipitation estimation methods and their impacts on hydrologic prediction in a
549 high latitude basin. *Journal Of Geophysical Research*, 117: D09108.
- 550 Yong, B. et al., 2010. Hydrologic evaluation of Multisatellite Precipitation Analysis
551 standard precipitation products in basins beyond its inclined latitude band: A case
552 study in Laohahe basin, China. *Water Resources Research*, 46(7): W07542.
- 553 Zak, S.K. and Beven, K.J., 1999. Equifinality, sensitivity and predictive uncertainty in the
554 estimation of critical loads. *The Science of The Total Environment*, 236(1-3):
555 191-214.
- 556 Zhao, R.J., 1992. The Xinanjiang model applied in China. *Journal Of Hydrology*, 135(1-
557 4): 371-381.
- 558 Zhao, R.J., Zhuang, Y.G., Fang, L.R., Liu, X.R. and Zhang, Q.S., 1980. The Xinanjiang
559 Model, *Hydrological Forecasting Proceedings Oxford Symposium*. IAHS
560 Publication, Oxford University, pp. 351-356.
- 561
- 562
- 563



1

2 **Figure 1** Wangchu Basin Map. (a) Location of Bhutan and the surrounding countries. (b)

3 Location of Wangchu Basin in Bhutan and its elevation. (c) Map of Wangchu Basin, rain

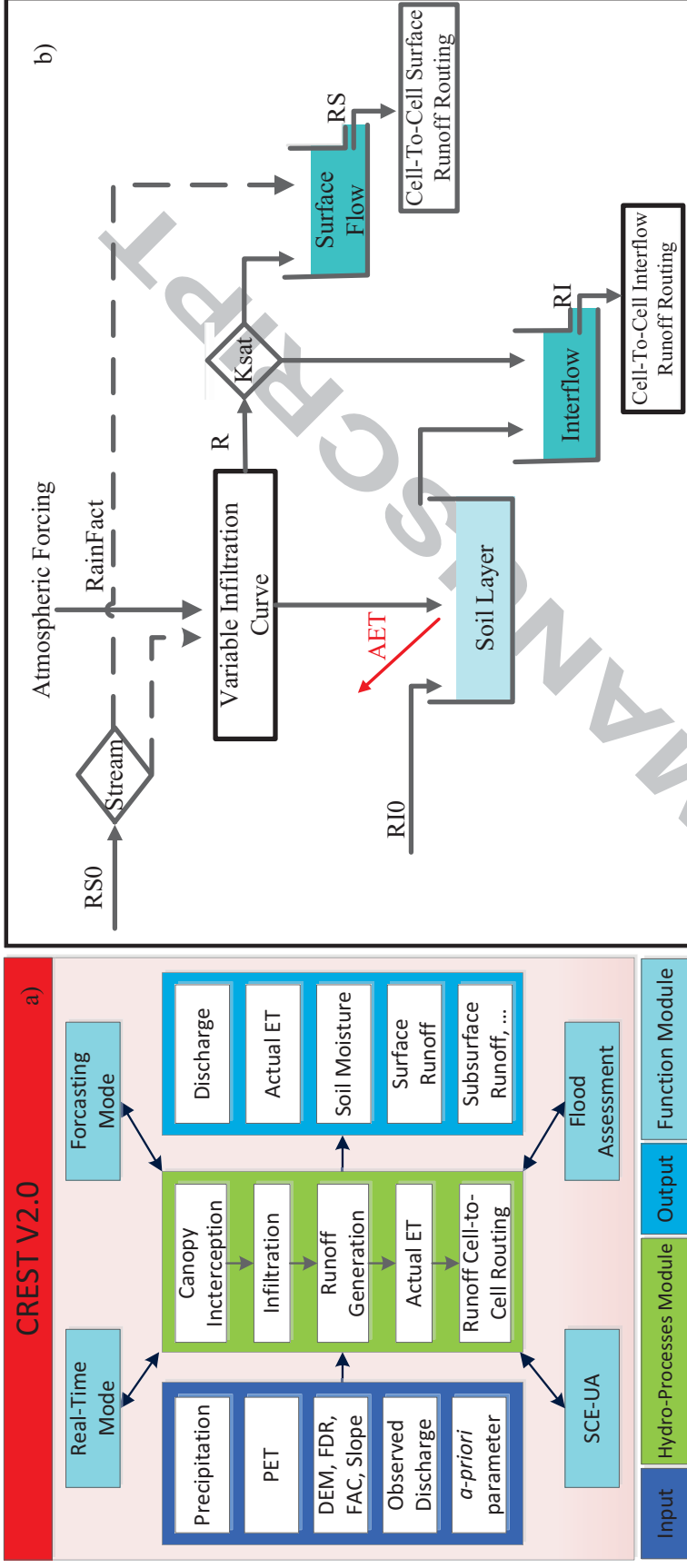
4 gauges, streamflow station, topography, Thiessen polygons applied to the rain gauge data

5 and the $0.25^{\circ} \times 0.25^{\circ}$ grids of the satellite rainfall estimates.

6

7

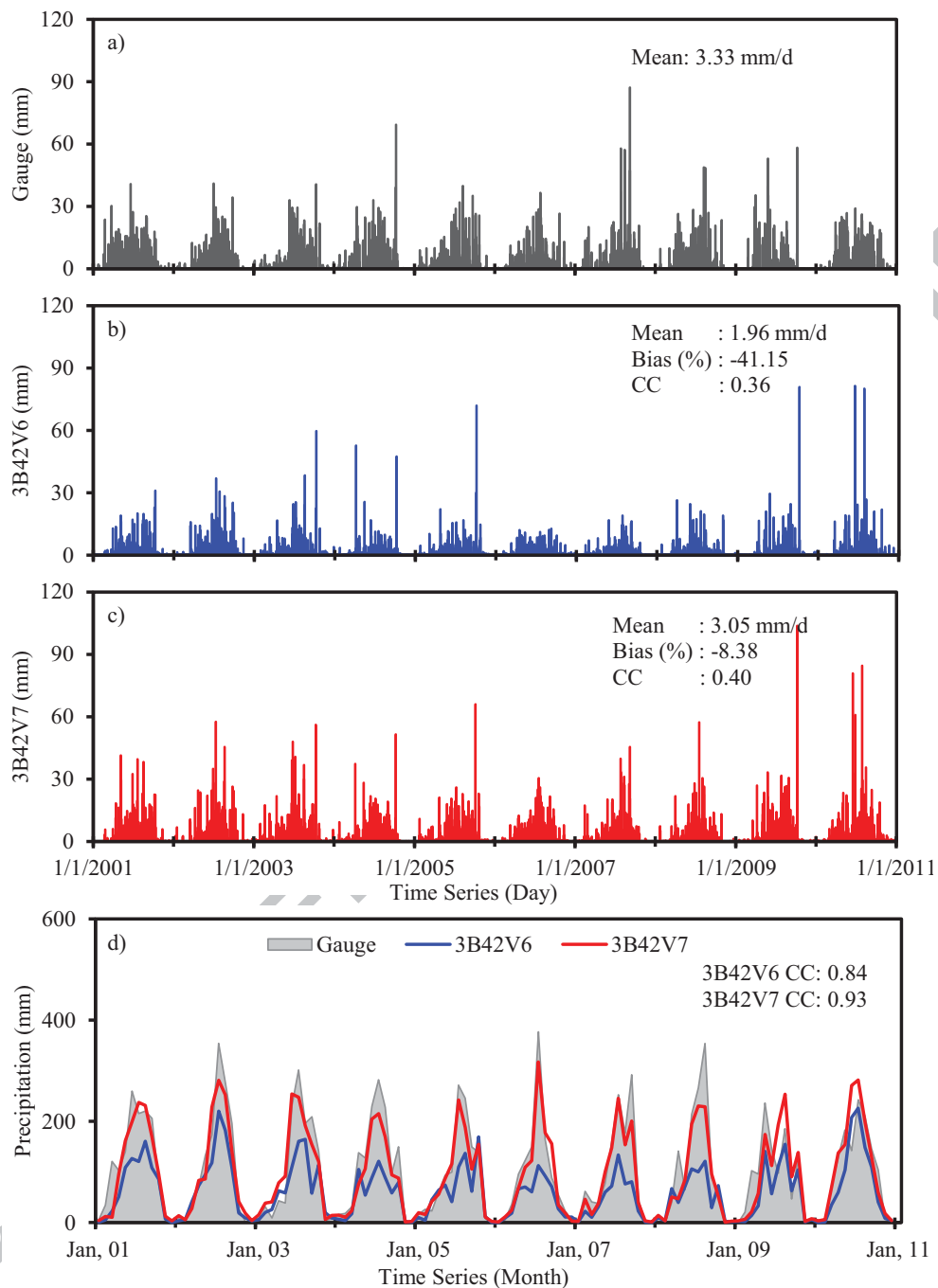
8



9

Figure 2 a) The framework of the CREST model version 2.0 and b) vertical profile of hydrological processes in a grid cell.

11



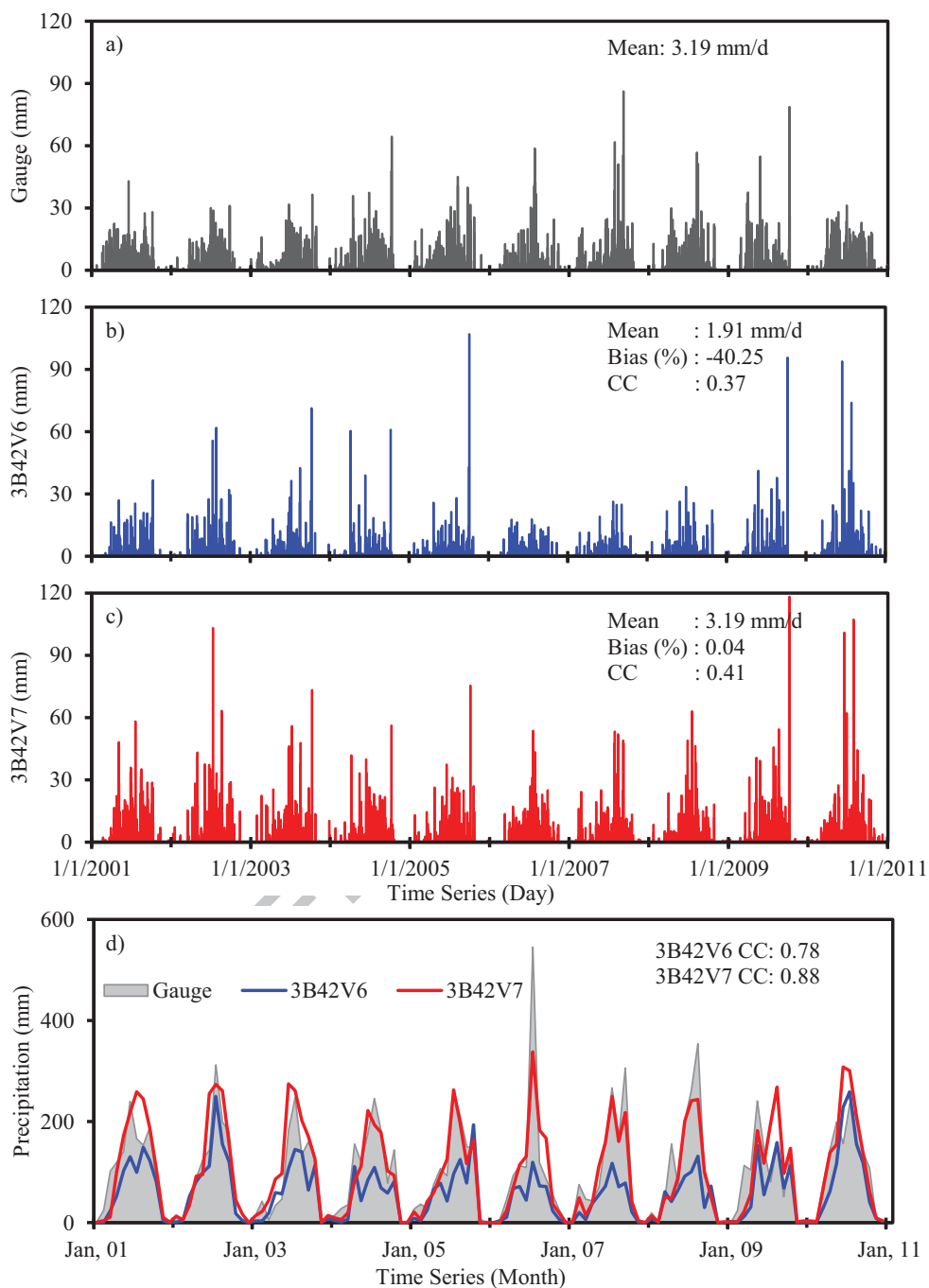
12

13 **Figure 3** Basin-averaged precipitation of a) Gauge, b) 3B42V6 and c) 3B42V7 for the

14 period January 2001-December 2010. Monthly data for both 3B42V6 and 3B42v7 are

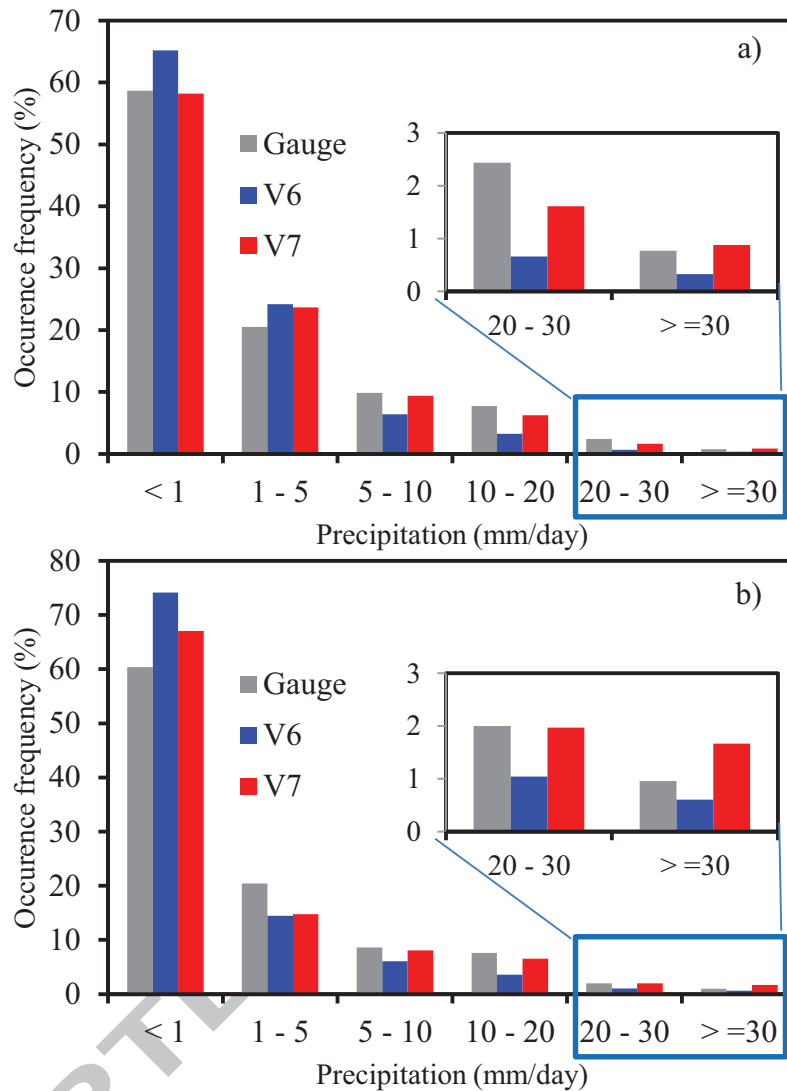
15

shown in d).



16
17 **Figure 4** As in Figure 3, but for a single grid cell (Grid32).

18



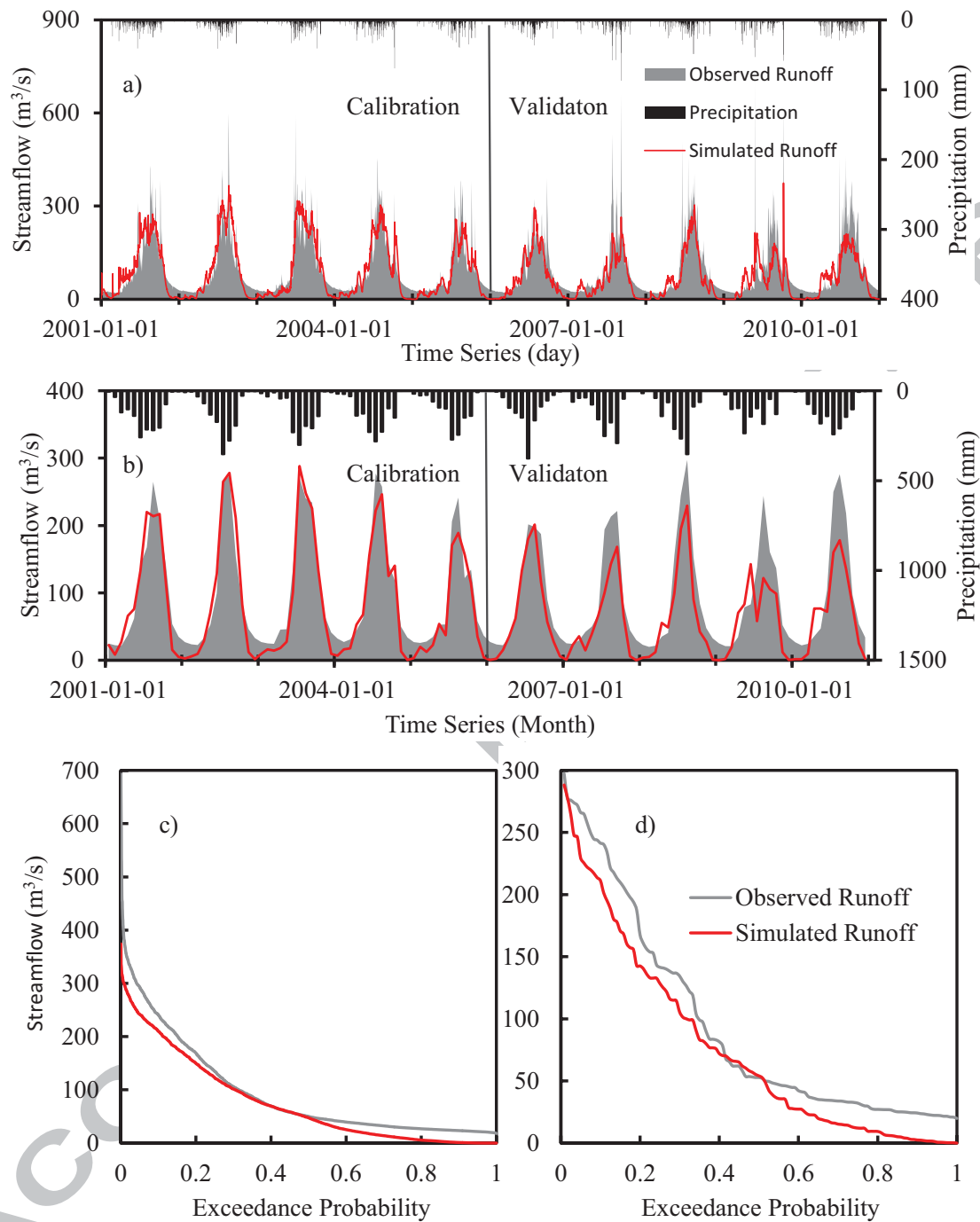
19

20 **Figure 5** Occurrence frequencies of rain gauge, 3B42V6 and 3B42V7 for a) basin-

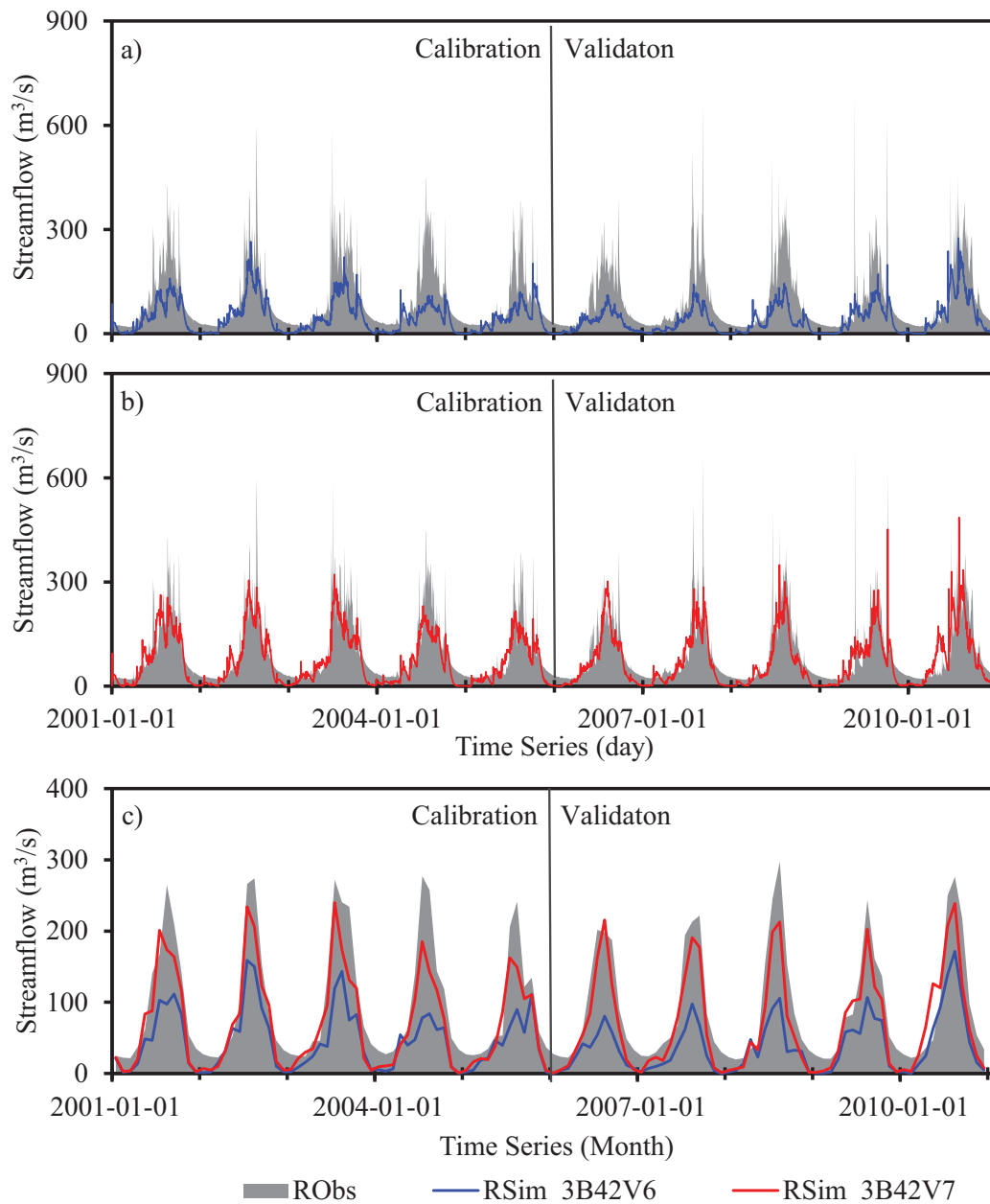
21

averaged data and b) single grid cell (Grid32).

22



23
 24 **Figure 6** Comparison of observed and simulated streamflow using gauge data as input: a)
 25 daily calibration (2001.1.1-2005.12.31) and validation (2006.1.1-2010.12.31), b) monthly
 26 data, c) exceedance probabilities using daily data from 2001.1.1 to 2010.12.31) and d)
 27 exceedance probabilities using monthly data.



28

29 **Figure 7** Comparison of CREST simulated streamflow from 3B42V6 (blue line) and

30 3B42V7 (red line) with gauge-calibrated parameters and observed stream flow in both

31 calibration (2001.1.1-20.5.12.31) and validation (2006.1.1-2010.12.31) period. a) Daily

32 data from 3B42V6; b) Daily data from 3B42V7; c) Monthly data from both 3B42V6 and

33

3B42V7.

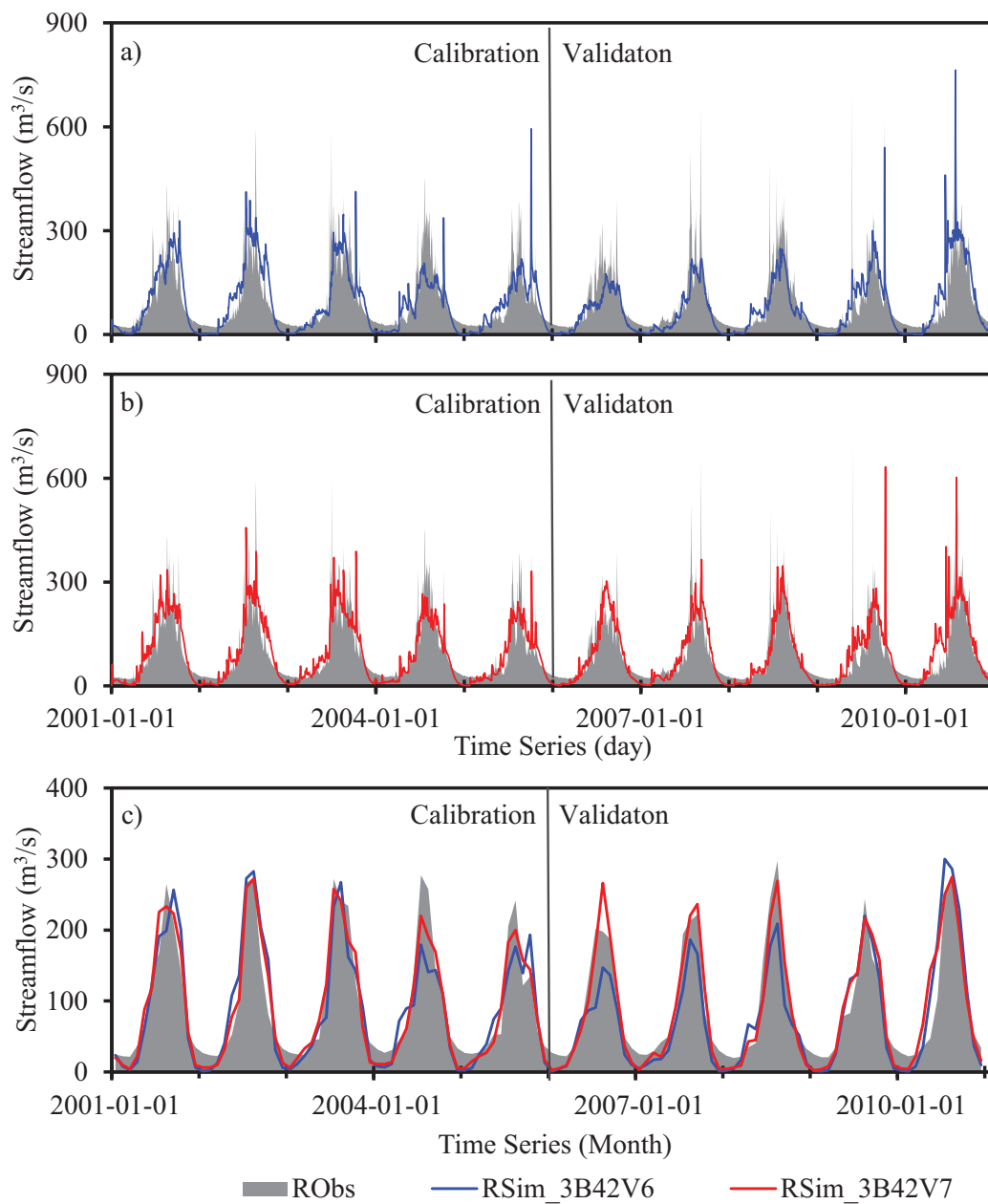
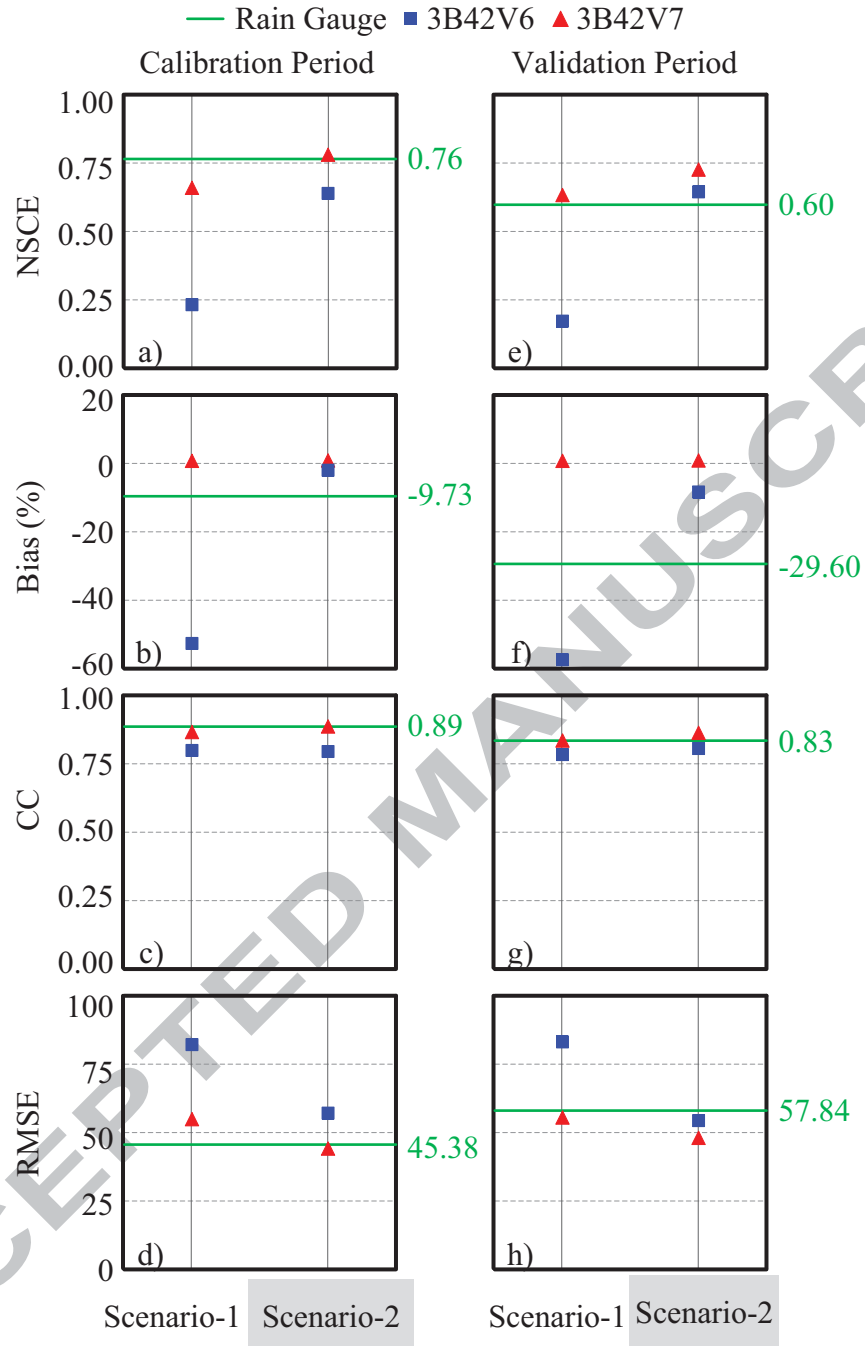


Figure 8 As in Figure 9, but the parameters were recalibrated using 3B42V6 and 3B42V7, respectively.



37

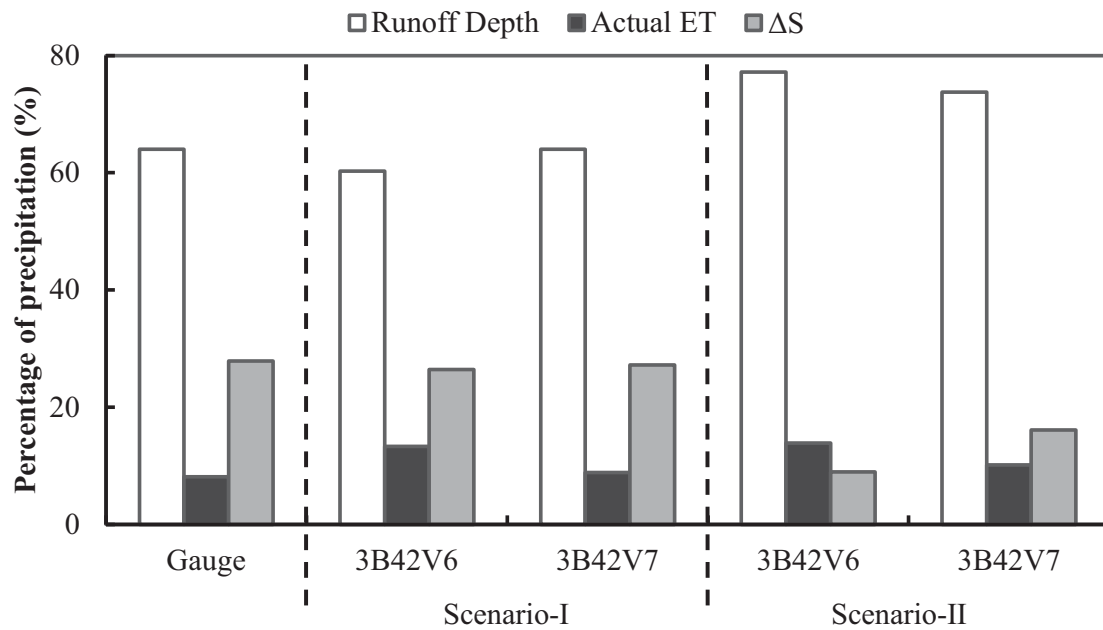
38 **Figure 9** Comparison of the streamflow performance statistics of the TPA 3B42V6 and

39 3B42V7 precipitation for the two simulation scenarios in both calibration period (a-d)

40

and validation period (e-h).

41



42

43 **Figure 10** Relative change of the water balance components using rain gauge and
 44 satellite rainfall based on ten-year annual averages (2001-2010) hydrological simulations
 45 in scenarios I and II

46

1 **Table 1** Monthly observed precipitation and runoff averaged from 2001 to 2010

Month	Rain Gauge (mm/month)					Streamflow Station
	Betikha	Dochula	Drukgyel Dzong	Namjayling Haa	DSC_Paro	Chhukha $\text{m}^3 \text{s}^{-1}$
Jan	14	19	0	12	8	26
Feb	49	18	9	24	18	23
Mar	176	17	26	33	15	25
Apr	346	53	29	54	34	38
May	368	105	60	69	57	55
Jun	390	279	123	124	81	111
Jul	<u>546</u>	359	185	183	<u>199</u>	222
Aug	383	<u>368</u>	<u>191</u>	<u>161</u>	103	<u>251</u>
Sep	326	217	108	120	77	180
Oct	182	116	71	77	63	109
Nov	10	11	3	4	3	52
Dec	4	9	1	2	1	34

2 **Table 2** Parameters to be calibrated in CREST V2.0, their description, ranges and default

3 values

Parameter	Description	Numeric Range	Default Value
Ksat	soil saturated hydraulic conductivity (mm/d)	0-2827.2	500
RainFact	multiplier on the precipitation field	0.5-1.2	1.0
WM	mean soil water capacity	80-200	120
B	exponent of the variable infiltration curve	0.05-1.5	0.25
IM	impervious area ratio	0-0.2	0.05
KE	ratio of the PET to actual evapotranspiration	0.1-1.5	1.0
coeM	overland runoff velocity coefficient	1-150	90
coeR	multiplier used to convert overland flow speed to channel flow speed	1-3	2
coeS	multiplier used to convert overland flow speed to interflow flow speed	0.001-1	0.3
KS	overland reservoir discharge parameter	0-1	0.6
KI	interflow reservoir discharge parameter	0-1	0.25

4

5 **Table 3** Comparison of daily observed and simulated streamflow under two calibration

6 scenarios

Precipitation Products	Scenario I				Scenario II			
	NSCE	Bias(%)	CC	RMSE	NSCE	Bias(%)	CC	RMSE
Calibration Period								
Gauge	0.76	-9.73	0.89	45.38	-	-	-	-
3B42V6	0.23	-52.94	0.80	81.99	0.63	-1.70	0.80	56.55
3B42V7	0.66	-26.98	0.86	54.65	0.78	-4.81	0.88	43.94
Validation Period								
Gauge	0.59	-29.59	0.83	57.85	-	-	-	-
3B42V6	0.17	-57.78	0.78	82.98	0.65	-8.67	0.81	54.00
3B42V7	0.63	-25.15	0.83	55.26	0.72	-3.02	0.86	47.72

7

Table 4 As in **Table 3**, but for monthly data

Precipitation Products	Scenario I				Scenario II			
	NSCE	Bias(%)	CC	RMSE	NSCE	Bias(%)	CC	RMSE
Calibration Period								
Gauge	0.91	-9.75	0.96	25.18	-	-	-	-
3B42V6	0.25	-53.01	0.88	72.08	0.75	-1.66	0.87	41.41
3B42V7	0.77	-27.06	0.94	39.76	0.91	-4.83	0.95	25.41
Validation Period								
Gauge	0.70	-29.59	0.88	43.63	-	-	-	-
3B42V6	0.19	-57.81	0.89	71.35	0.79	-8.65	0.89	36.29
3B42V7	0.80	-25.25	0.94	35.58	0.89	-3.08	0.95	26.53

8 **Table 5** CREST model parameter values calibrated with different precipitation inputs for
9 the calibration period of January 2001-December 2005

Parameters	Gauge	3B42V6	3B42V7
RainFact	0.87	1.34	0.98
Ksat	56.90	33.09	52.73
WM	166.50	142.71	166.52
B	1.48	1.48	1.48
IM	0.20	0.20	0.20
KE	0.10	0.05	0.13
coeM	88.05	63.67	67.95
coeR	2.68	1.33	1.44
coeS	0.43	0.47	0.67
KS	0.99	0.71	0.78
KI	0.20	0.13	0.14

10

Highlights

Comprehensively evaluated the latest satellite precipitation algorithm TMPA V6 and V7

The new V7 provides more accurate spatiotemporal distribution than its predecessor V6

V7 also provides improved hydrologic utility even without conventional recalibration

Promising potential application of the latest V7 in ungauged basins across the world